McNamara, D. P., Beach, M. A., & Fletcher, P. N. (2002). Wideband analysis of indoor MIMO channels. (pp. 13 p). (COST 273), (TD (02) 026).

EUROPEAN COOPERATION
IN THE FIELD OF SCIENTIFIC
AND TECHNICAL RESEARCH

EURO-COST

SOURCE: Centre for Communications Research,
University of Bristol, UK.

COST 273 TD(02)026
Guildford, UK
January 17-18, 2002

Wideband Analysis of Indoor MIMO Channels

D.P. McNamara, M.A. Beach & P.N. Fletcher
Queen's Building,
University Walk, Clifton,
Bristol.
BS8 1TR. UK.
Phone: +44 117 928 8617
Fax: +44 117 954 5206
Email: Darren.McNamara@bristol.ac.uk

Wideband Analysis of Indoor MIMO Channels

D.P. McNamara*, M.A. Beach & P.N. Fletcher

Abstract

The application of MIMO communication systems in real environments will invariably require systems to operate over wideband channels. Although suitable techniques for processing wideband MIMO channels have been reported, their evaluation has mainly been based on simulation using modelled channels. In this paper we investigate some of the properties of wideband MIMO channels and compare the characteristics of simulated channels with those measured in indoor environments at 5.2GHz.

1 Introduction

The initial analysis of multiple-input multiple-output (MIMO) communication systems, along with algorithms for their exploitation, has mostly concentrated on narrowband systems [1]–[4]. Although much work still continues in this area, the narrowband requirement is a factor that would limit the deployment and application of these techniques in practical environments. In order to overcome this limitation, many of the common techniques for communication over wideband single-input, single-output (SISO) channels can be extended to MIMO systems. Examples of such extensions include equalisation [5], spread spectrum techniques [6] and orthogonal frequency division multiplexing (OFDM) [7]. The measurement and analysis of wideband MIMO channels is therefore beneficial to the development of these systems, both through direct system simulation using measured channel data, and through the development of wideband channel models.

To date, although many MIMO measurement campaigns have been reported in the literature, these have mostly investigated parameters such as narrowband channel capacity, spatial correlation, or other similar properties [8][9][10]. In these campaigns, even though wideband data has often been recorded, narrowband responses have been extracted for the subsequent analysis [9][10]. More recently, some investigation of wideband MIMO channels has been conducted [11]–[15]. Although these have proposed various channel models, there is still a requirement for further examination of measurement data in order to assess the properties of wideband MIMO channels and aid model development.

This paper describes the analysis of wideband MIMO channel responses recorded over a bandwidth of 120MHz at 5.2GHz. These campaigns have been conducted in a variety of indoor environments and with various array architectures and element types. The capacity of these channels has been evaluated for varying bandwidths and compared against that of channels generated from a stochastic model.

2 Measurement system and environments

The measurement platform used for these measurements is based on a Medav RUSK BRI vector channel sounder [16]. The transmitter employs a periodic multi-tone signal with a bandwidth

*Centre for Communications Research, University of Bristol, UK. *Email: Darren.McNamara@bristol.ac.uk.*

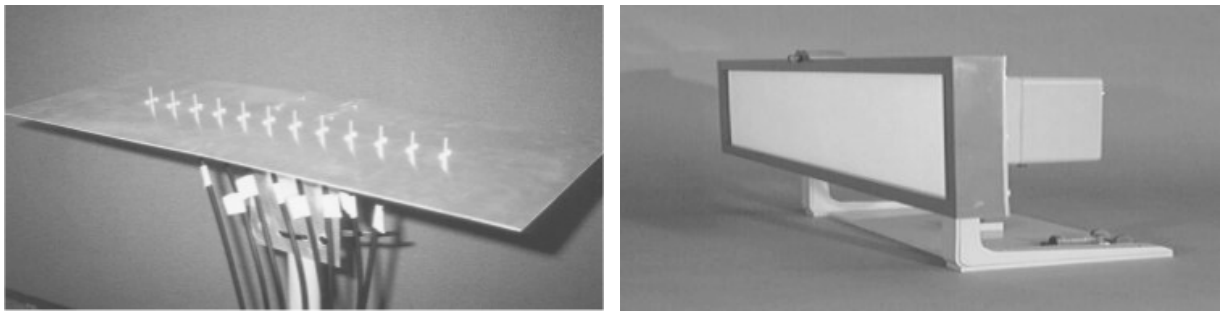

Figure 1: Arrays used during measurement campaigns.

of 120MHz centred at 5.2GHz and period of 0.8μs. This signal is constructed so that all tones have equal power and are evenly spaced over the measurement bandwidth. With the digital-to-analogue converter operating at 320MHz, the above parameters correspond to the transmission of 97 tones, each spaced by 1.25MHz. The periodic nature of this signal allows the determination of the channel's frequency response through a discrete fourier transform of one period of data sampled at the receiver. It is then only the useful 97 (complex) samples of this frequency domain data that are stored to disc for subsequent post-processing. Channel impulse responses can be estimated by suitable windowing and fourier transformation of the stored data.

Measurement time and frequency accuracy is assured through the use of rubidium referenced clocks at both transmitter and receiver, with a cable connection to provide absolute phase coherence. A back-to-back system calibration is conducted before the commencement of measurements to remove the effect of amplitude and phase distortions in the hardware and to provide a synchronisation reference for the determination absolute time-of-flight information.

The standard receiver in the Medav RUSK BRI is capable of measuring channel responses from up to 8 elements (for a single transmitter) by utilising a fast multiplexing system to switch between each element in turn. With the system configured to use a signal period of 0.8μs, one measurement from all receive elements is recorded in 12.8μs. MIMO channel sounding is achieved through the use of additional custom switching and synchronisation circuitry to control a second array at the transmitter that can also consist of up to 8 elements. For each transmit element in turn, a measurement is taken from each channel at the receiver. In this way, the complex channel responses of all 64 combinations of the eight transmit and eight receive elements are recorded to form the full MIMO channel response. Each complete 'MIMO snapshot' of the channel is therefore recorded in 102.4μs, which has been shown to be fast enough in the indoor environments under consideration to ensure that the channel remains stationary for the duration of each measurement [10].

For the analysis contained in this paper, data has been selected from various measurement campaigns conducted in different indoor environments and using various antenna arrays (previously reported in [17][18]). These arrays and environments are shown in Figures 1&2 respectively.

3 Wideband MIMO channels

3.1 Definitions

We define a MIMO channel response to be composed of the transfer functions between n_T transmit and n_R receive elements which, for a narrowband channel, can be represented by an $n_R \times n_T$ matrix, G. Each entry G_{jk} of this matrix is the complex transmission coefficient between element

Figure 2: Two of the environments in which channel measurements have been recorded.

$j \in [1, \ldots, n_R]$ at the receiver and element $k \in [1, \ldots, n_T]$ at the transmitter.

For a wideband channel, the response can be represented (in the time domain) as a tapped delay line

$$G(\tau) = \sum_{l=1}^{M} G_l \, \delta(\tau - \tau_l), \tag{1}$$

where G_l is the $n_R \times n_T$ channel response at delay τ_l and $M = \max\{L_{jk}\}$, $\forall j, k$, where L_{jk} is the excess delay for the channel between elements j and k (since it is not assumed that the component SISO channels all have the same maximum delay). Note that herein, we will use $G_{jk,l}$ to identify the complex transmission coefficient between elements j and k at delay l.

It is also useful to be able to consider the wideband MIMO channel in the frequency domain, particularly for the purposes of channel response normalisation (to remove the average pathloss, in both space and frequency) and for the calculation of channel capacity. (It is noted though that normalisation is not always appropriate since the variation in average pathloss also has a large effect on the performance of these systems [19]).

We define the equivalent frequency domain representation of the MIMO channel response in (1) to be given by the set of $n_R \times n_T$ matrices $\mathcal{G}_f$ for $f = 1, \ldots, F$, where $\mathcal{G}_{jk,f}$, for $f = 1, \ldots, F$, is the Fourier transform of the impulse response $G_{jk,l}$, for $l = 1, \ldots, M$.

Normalisation of the wideband channel response, can be accomplished by an extension of the narrowband normalisation process to include the frequency domain so that the normalised matrix response (in the frequency domain), $\mathcal{H}$, is given by

$$\mathcal{H} = \frac{\mathcal{G}}{\sqrt{\frac{\sum_{j=1}^{n_R} \sum_{k=1}^{n_T} \sum_{f=1}^{F} |\mathcal{G}_{jk,f}|^2}{n_R n_T F}}}, \tag{2}$$

where the denominator is the average pathloss in both space and frequency.

3.2 Wideband stochastic MIMO model

Previous reports of the simulation and modelling of wideband MIMO systems have employed various models to generate the MIMO channel response, G. We include a description here of a simple stochastic model [7][20] of these channels in ideal rich scattering Rayleigh environments, for comparison against the measured data. The model is defined as follows (where E denotes expectation and * indicates complex conjugation):

• All elements of G_l are samples of i.i.d. zero-mean complex Gaussian random processes such that $E\{G_{j_1 k_1, l}\,,\, G^*_{j_2 k_2, l}\} = 0$, for $j_1 \neq j_2$ or $k_1 \neq k_2$, and $\forall\, l$.

• The channel coefficients comprising G_l are uncorrelated from one delay to another such that $E\{G_{jk,l_1}\,,\, G^*_{jk,l_2}\} = 0$, for $l_1 \neq l_2$ and $\forall\, j, k$.

• The mean power of G_l for a given delay, $P_l = E\{|G_{jk,l}|^2\}$, $\forall j, k$, is either given by an exponential power delay profile (PDP) or one selected from the various profiles published for different standards. For the simulations reported here, we will use the PDP defined by Hiperlan/2 channel model 'A' (small indoor office) [21], which has an r.m.s. delay spread of 50ns.

3.3 Capacity of wideband MIMO channels

When a transmission is sent through a (narrowband) fading, single-input single-output (SISO) bandlimited channel, in the presence of additive white gaussian noise (AWGN), the channel capacity is given by

$$C = W \log_2 \left(1 + \rho\,|\mathcal{H}|^2\right) \quad \text{bits/s}, \tag{3}$$

where W is the channel bandwidth, ρ is the average signal to noise ratio at the receiver and $\mathcal{H}$ is the normalised channel response [22].

It has been shown in [2][3] that (3) can be extended to encompass multiple-input multiple-output (MIMO) channels so that the expression for channel capacity becomes, (in a frequency-flat fading environment),

$$C = W.\log_2 \left(\det\left(I_{n_R} + \frac{\rho}{n_T}\mathcal{H}\mathcal{H}^\dagger\right)\right) \quad \text{bits/s}, \tag{4}$$

where I_{n_R} is the $n_R \times n_R$ identity matrix, ρ is the average signal to noise ratio at each receiver branch, $\mathcal{H}$ is the $n_R \times n_T$ normalised narrowband channel response matrix, det is the determinant operator and $\dagger$ is hermitian transpose. (Note that this is for the case where the transmitter has no knowledge of the channel response coefficients [3]).

The capacity of a wideband channel can be obtained by integrating (4) over the bandwidth of interest, which can be expressed in discrete form as

$$C_W = \lim_{R\to\infty,\Delta f\to 0} \sum_{f=1}^{R} \Delta f \log_2 \left(\det\left(I_{n_R} + \frac{\rho}{n_T}\mathcal{H}_f\mathcal{H}_f^\dagger\right)\right) \quad \text{bits/s}, \tag{5}$$

where $\Delta f = W/R$ and $\mathcal{H}_f$ is the $n_R \times n_T$ narrowband channel response matrix at frequency f, and where ρ is now the average signal to noise ratio over the whole bandwidth, W. Expressing the integration in this form is useful here since the channel measurement data consists of discrete frequency samples spaced by $\Delta f = 1.25$MHz, hence allowing easy calculation of capacity. The capacity at differing bandwidths can then be calculated by selection of the value of R.

Since (4) assumes a frequency flat propagation environment, the capacity is not dependant on frequency and hence is usually normalised by W to obtain the normalised capacity (or spectral efficiency) of the channel. Although this is still possible for wideband channels, it results in a *mean* spectral efficiency over the bandwidth of interest since capacity is now a function of the frequency band over which it is calculated.

As shown, the expressions in (3)–(5) give the channel capacity for a fixed signal to noise ratio, ρ. However, this does not give a fair comparison between channels of different bandwidths since $\rho = P/(WN_0)$, where P is the average received power and N_0 is the noise power spectral density at the receiver. Since the noise power increases with bandwidth, the input power to the channel must also be increased in proportion to the bandwidth in order to maintain a constant ρ. A more realistic assumption is therefore to evaluate the capacity of channels having different bandwidths

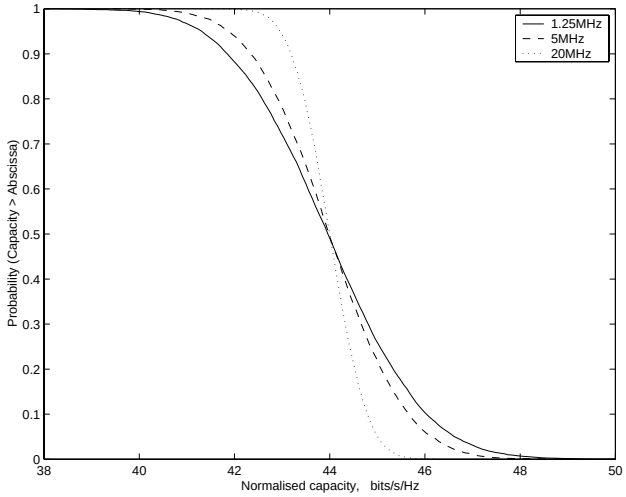

Figure 3: Normalised capacity CCDFs for simulated (8x8) MIMO channels with bandwidths of 1.25, 5 and 20MHz and for ρ fixed at 20dB.

for a fixed average receive power, P. Hence, replacing ρ in (5) gives

$$C_W = \lim_{R\to\infty,\Delta f\to 0} \sum_{f=1}^{R} \Delta f \log_2 \left(\det \left(I_{n_R} + \frac{P}{n_T W N_0} \mathcal{H}_f \mathcal{H}_f^{\dagger} \right) \right) \quad \text{bits/s}, \tag{6}$$

where each term of the summation is now a function of the overall bandwidth. (It is again assumed that the transmitter does not have any knowledge of the channel response and therefore cannot preferentially allocate power to those frequencies which achieve the highest capacities.)

4 Simulation and data analysis

4.1 Capacity of simulated channels

We first investigate the capacities of wideband MIMO channels generated according to the model described in Section 3.2 (employing the PDP specified by Hiperlan/2 channel model 'A'). For each simulation, 10,000 channels are created, transformed to their frequency domain representation and normalised according to (2), before calculating their capacities at the required bandwidth. We use the notation (n_R, n_T) to denote the dimensions of the MIMO system being investigated.

Figure 3 shows the complementary cumulative distribution functions (CCDFs) of normalised capacity for (8,8) channels of varying bandwidths and with a fixed signal to noise ratio, ρ, of 20dB. As the bandwidth is increased it can be seen that the mean normalised capacity remains roughly constant, while the variance significantly reduces. Therefore, whilst there is a much lower probability of achieving the highest capacities, for small outage probabilities the normalised capacity has increased. This effect is due to the increasingly frequency selective nature of the channel as the bandwidth becomes larger, resulting in frequency diversity. Hence, for channels with a bandwidth much greater than the coherence bandwidth, there should only be a small variation in normalised capacity between different channel realisations (given ideal spatial decorrelation).

A different result is obtained if the constant receive power constraint is used instead of a constant signal to noise ratio. This comparison can be seen in Figure 4a which shows the normalised capacity reducing as the bandwidth is increased and the receive power remains constant. (In practice, rather

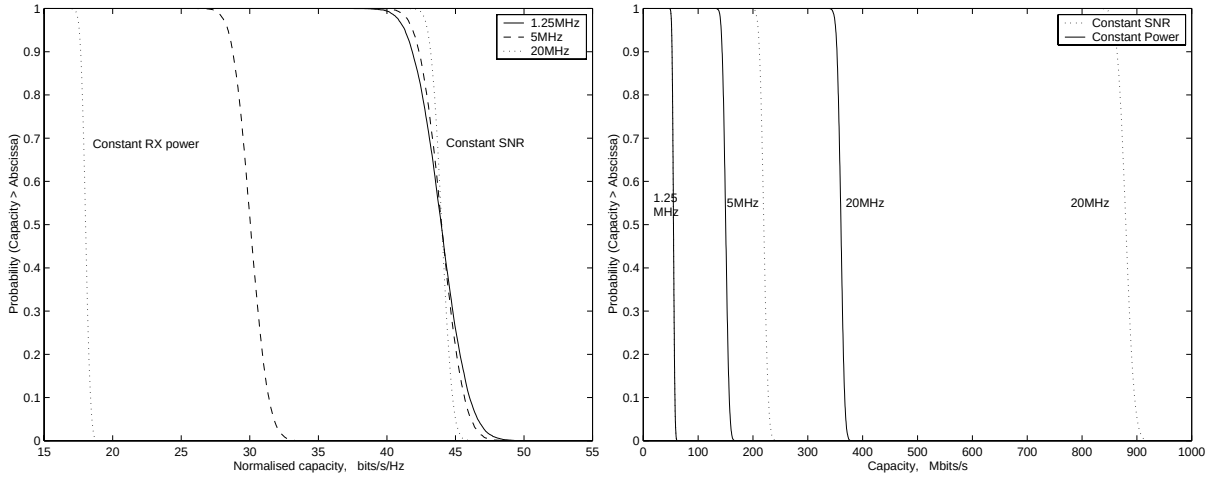

(a) Normalised capacity

(b) Absolute capacity

Figure 4: Capacity CCDFs for simulated (8x8) MIMO channels with bandwidths of 1.25, 5 and 20MHz. Comparison is shown between capacities calculated for a fixed ρ and for a fixed average receive power ($\rho_N = 20$dB).

than define a constant average receive power, P, we define a fixed *narrowband signal to noise ratio*, ρ_N, for a bandwidth of Δf. Hence, the signal to noise ratio varies such that $\rho = \rho_N.(W/\Delta f)$).

Similarly, this reduction in spectral efficiency with increasing bandwidth can be noted from Figure 4b and more readily from Figure 5 where for each step expansion in bandwidth the increase in capacity becomes smaller. This illustrates that evaluating the performance of channels of varying bandwidth for a constant signal to noise ratio and using normalised capacity as the metric can produce misleading results.

4.2 Analysis of measured channels

Initially, we analyse data collected in a large open office that has been emptied of all furniture (see Figure 2 and [17]). Previous analysis has shown this environment to produce high levels of multipath scattering and also to have a reasonably high mean r.m.s. delay spread of about 30ns.

The comparison of normalised capacity between measured and simulated channels is shown in Figure 6a. It can immediately be seen that as expected the measured channels achieve lower capacities than those generated from the idealised model. This is even more pronounced when comparing absolute capacity (Figure 6b) since any difference in normalised capacity is now multiplied by the bandwidth. Hence as bandwidth increases, the discrepancy between measured and simulated channels increases. So where the difference is only 14Mbits/s at 1.25MHz bandwidth, it is 128Mbits/s at 20MHz bandwidth (for a 10% outage).

In contrast to the simulated channels, variation amongst the plots of normalised capacity for different bandwidths of the measured channels is very small (Figure 6a). As the bandwidth increases, although the probability of achieving the highest capacities reduces slightly, almost no change is discernable for the lower capacities. Figure 7 shows this result to be a function of the dimension of the MIMO system, since for lower numbers of antenna elements, changes in bandwidth effect a larger influence on the normalised capacity. This is likely to be due to the reduced spatial diversity experienced by systems of small dimension. As the bandwidth of these channels is increased, the additional frequency diversity is of greater benefit than it would be to a system which exhibits

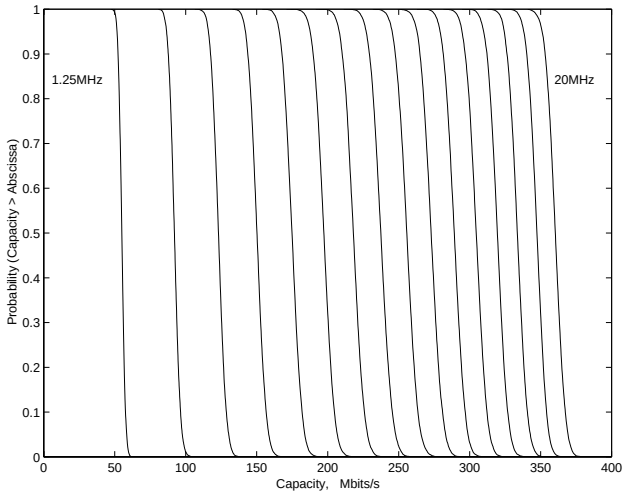

Figure 5: Capacity CCDFs for simulated (8x8) MIMO channels with the bandwidth increased in 1.25MHz steps between 1.25 and 20MHz, and with a fixed average receive power ($\rho_N = 20$dB).

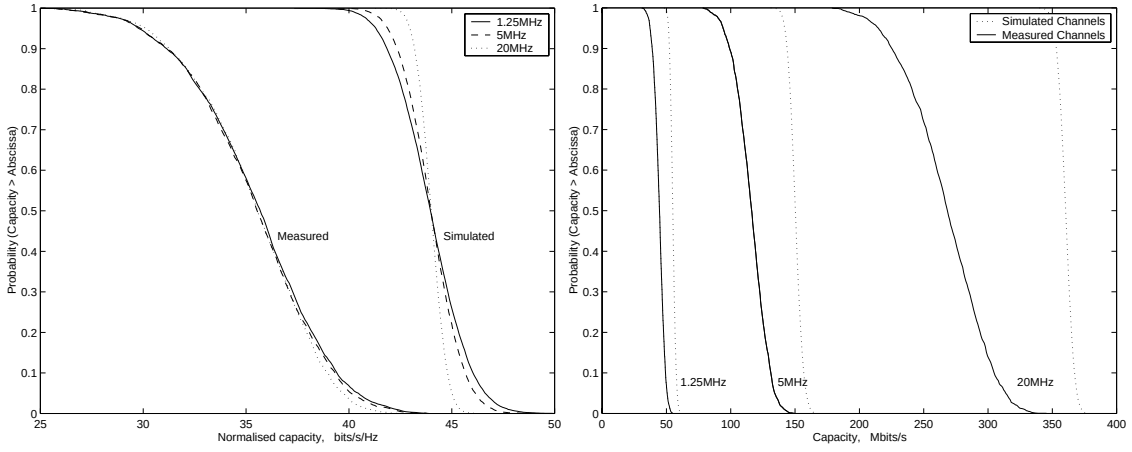

(a) Normalised capacity (b) Absolute capacity

Figure 6: Comparison between capacity CCDFs for (8x8) measured and simulated MIMO channels with bandwidths of 1.25, 5 and 20MHz. (a) Normalised capacity for ρ fixed at 20dB. (b) Absolute capacity for a fixed average receive power ($\rho_N = 20$dB).

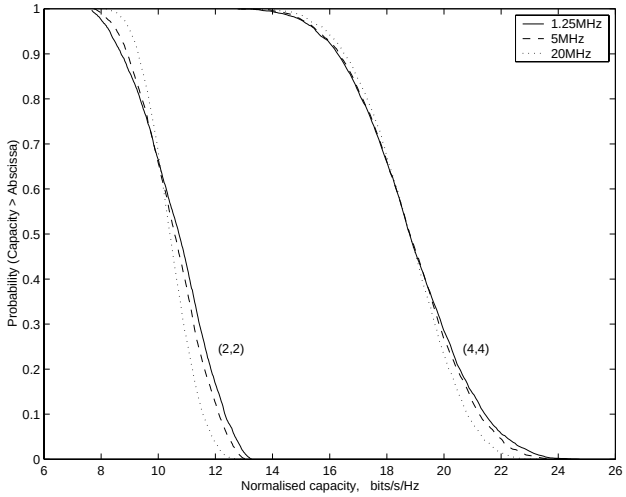

Figure 7: Normalised capacity CCDFs for (2,2) and (4,4) measured MIMO channels with bandwidths of 1.25, 5 and 20MHz and for ρ fixed at 20dB.

higher spatial diversity.

In order to bring the characteristics of the modelled channels closer to those of measured channels, it is obviously necessary to introduce spatial correlation amongst the array elements. For a wideband channel though, it is not clear whether spatial correlation should be introduced for just the first matrix tap of the impulse response (where a dominant, possibly line of sight, path may be expected), for all taps equally, or to have a different degree of correlation for each tap. We now investigate this for some of the measured channel response data.

Figure 8 gives an example of one (8,8) wideband MIMO channel response measured in a populated office (see Figure 2 and [18]). Each of the 64 component SISO impulse responses are shown side by side, all having been normalised by the peak response of any of the transmission coefficients ($\max(|G_{jk,l}|)$, $\forall\, j,k,l$), and then a threshold applied at -30dB. (For this measured channel data, samples of the impulse responses are separated by 8.3ns). Although it can be seen all SISO impulse responses have similar distributions of power with delay, some spatial correlation can be noted from slight periodic variation in the responses as element index increases.

In order to quantitatively assess the inter-element correlation, for each $n_R \times n_T$ matrix tap, G_l, of the MIMO impulse response, the cross-correlations between all 64 transmission coefficients have been calculated over several hundred channel realisations. The result is shown in Figure 9, with one plot for each of the first 6 delay taps. Within each plot every 'square' of 8×8 values represents the cross-correlation between one element, G_{jk}, and all others. Therefore, the top-left square displays the correlation between G_{11} and all other elements and the top-right square displays the correlation between G_{18} and all other elements.

Starting with the first delay tap, shown in Figure 9a, it can be seen that within each 8×8 'square' there is a region of high correlation between the appropriate reference element, G_{jk}, and the elements surrounding it. This indicates that there is a high correlation between transmission coefficients for adjacent elements, which reduces as the elements increase in separation. In this example, the correlation amongst elements at the transmitter and amongst elements at the receiver is roughly equal since the correlation coefficients decay evenly in both the vertical and horizontal directions. Other examples illustrating high correlation at solely the transmit or receive array have also been measured, but are not shown here for brevity.

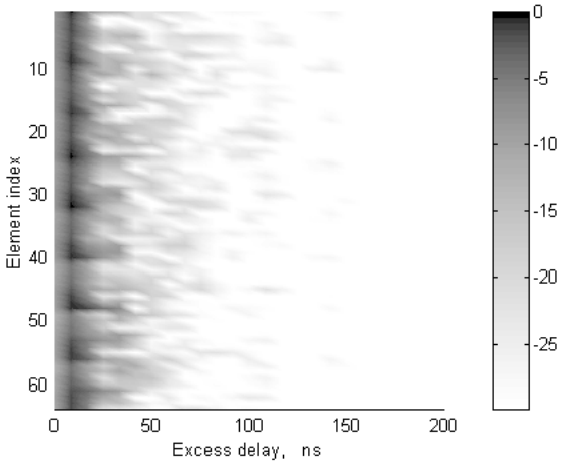

Figure 8: An example channel impulse response for a measured (8,8) MIMO channel. 'Element index' indicates one of the 64 SISO component channels constituting the overall MIMO response.

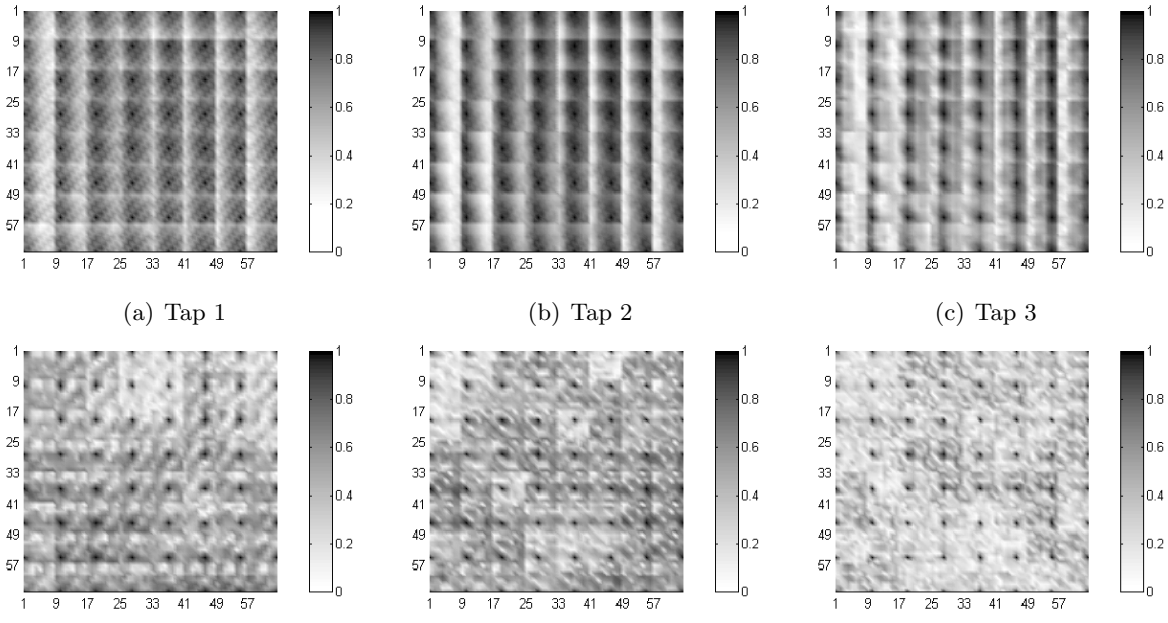

(a) Tap 1 (b) Tap 2 (c) Tap 3

(d) Tap 4 (e) Tap 5 (f) Tap 6

Figure 9: Cross-correlation coefficients between each element of the channel response matrix, and all others. (a) to (f) show the matrices of coefficients for the first 6 taps of the impulse response.

Correlation amongst adjacent elements can be seen to increase for the second delay tap (Figure 9b). This then reduces as the delay increases, so that by tap 6 it can be seen that there are 64 peaks showing the auto-correlation for each transmission coefficient, but all other values representing the cross-correlations are much lower, with a mean of 0.16.

As noted above, similar results have been obtained for other environments, antenna configurations and system configurations. For each scenario, different correlation patterns are generated depending on the spatial correlation at both the transmit and receive arrays. In general though, for the channel measurement data investigated so far, the correlation between transmission coefficients for each matrix tap of the impulse response appears to follow the same trend as the example shown here.

Although the work reported here only outlines an initial investigation into wideband MIMO channels, current analysis is continuing to look at the distribution of these characteristics. The results from this can then be combined with an enhanced model to include spatial correlation, with the aim of bringing the performance and characteristics of simulated channels closer to those of real environments.

5 Conclusions

The capacity variation of wideband MIMO channels has been investigated for both a constant signal to noise ratio and for a constant received power constraint and the difference that these two constraints make to the performance comparison of these channels has been illustrated.

The capacity of simulated channels has been compared against that of measured wideband MIMO channels. In general it has been shown how an increase in bandwidth provides frequency diversity resulting in a reduction in the variance of normalised capacity. For measured channels though, it was noted that for the (8,8) system, varying bandwidth made little difference to the normalised capacity. However, as the dimension of the MIMO system was reduced, changes in bandwidth exerted a greater influence on the capacity, indicating that MIMO systems with small numbers of antennas may gain the most from exploiting wideband channels since they experience less spatial diversity.

An appreciable difference between the capacities achieved by measured and simulated channels was also shown. This was mainly attributed to the model employed here not including any spatial correlation. Hence, some of the measured data was analysed in order to ascertain how correlation between elements of the channel response matrix varies with the taps of the impulse response. This information will now provide input for continuing work to produce an enhanced model to incorporate spatial correlation.

Acknowledgments

The authors gratefully acknowledge the financial contribution of the UK EPSRC, HEFCE (JREI '98), QinetiQ Ltd. and the IST SATURN project for their support of parts of this work.

References

[1] G.J. Foschini, "Layered Space-Time Architecture for Wireless Communication in a Fading Environment When Using Multiple Antennas," *Bell Labs. Tech. Journal*, vol. 1, no. 2, pp. 41–59, 1996.

[2] G.J. Foschini and M.J. Gans, "On Limits of Wireless Communications in a Fading Environment When Using Multiple Antennas," *Wireless Personal Communications*, vol. 6, no. 3, pp. 311, Mar. 1998.

[3] I. Telatar, "Capacity of Multi-Antenna Gaussian Channels," *European Trans. on Telecommunications*, vol. 10, no. 6, Nov. 1999.

[4] V. Tarokh, N. Seshadri, and A.R. Calderbank, "Space-Time Codes for High Data Rate Wireless Communication: Performance Criterion and Code Construction," *IEEE Trans. on Inform. Theory*, vol. 44, no. 2, pp. 744–765, Mar. 1998.

[5] A. Lozano and C. Papadias, "Space-Time Receiver for Wideband BLAST in Rich-Scattering Wireless Channels," in *IEEE Conf. on Veh. Technol.*, May 2000, Tokyo.

[6] H. Huang, H. Viswanathan, and G.J. Foschini, "Achieving High Data Rates in CDMA Systems Using BLAST Techniques," in *IEEE Globecom*, Nov. 1999.

[7] R.J. Piechocki, P.N. Fletcher, A.R. Nix, C.N. Canagarajah, and J.P. McGeehan, "Performance Evaluation of BLAST-OFDM Enhanced Hiperlan/2 Using Simulated and Measured Channel Data," *IEE Electronics Letters*, vol. 37, no. 18, pp. 1137–1139, Aug. 2001.

[8] C.C. Martin, J.H. Winters, and N.R. Sollenberger, "Multiple-Input Multiple-Output Radio Channel Measurements," in *IEEE Conf. on Veh. Technol.*, Oct. 2000, Boston.

[9] J.P. Kermoal, L. Schumacher, P.E. Mogensen, and K.I. Pedersen, "Experimental Investigation of Correlation Properties of MIMO Radio Channels for Indoor Picocell Scenarios," in *IEEE Conf. on Veh. Technol.*, Oct. 2000, Boston.

[10] D.P. McNamara, M.A. Beach, and P.N. Fletcher, "Experimental Investigation of the Temporal Variation of MIMO Channels," in *IEEE Conf. on Veh. Technol.*, Oct. 2001, Atlantic City.

[11] A.F. Molisch, M. Steinbauer, M. Toeltsch, E. Bonek, and R.S. Thoma, "Measurement of the Capacity of MIMO systems in Frequency Selective Channels," in *IEEE Conf. on Veh. Technol.*, May 2001, Rhodes.

[12] H. Bolcskei, D. Gesbert, and A.J. Paulraj, "On the Capacity of Wireless Systems Employing OFDM-based Spatial Multiplexing," Submitted to IEEE Trans. Commun.

[13] K.I. Pedersen, J.B. Anderson, J.P. Kermoal, and P. Mogensen, "A Stochastic Multiple-Input Multiple-Output Radio Channel Model for Evaluation of Space-Time Coding Algorithms," in *IEEE Conf. on Veh. Technol.*, Oct. 2000, Boston.

[14] M. Stege, J. Jelitto, M. Bronzel, and G. Fettweis, "A Multiple-Input Multiple-Output Channel Model for Simulation of TX and RX Diversity Systems," in *IEEE Conf. on Veh. Technol.*, Oct. 2000, Boston.

[15] R.R. Muller, "A Random Matrix Model of Communication via Antenna Arrays," Submitted to IEEE Trans. Info. Theory.

[16] R.S. Thoma, D. Hampicke, A. Richter, G. Sommerkorn, A. Schneider, U. Trautwein, and W. Wirnitzer, "Identification of Time-Variant Directional Mobile Radio Channels," *IEEE Trans. on Instrum. Meas.*, vol. 49, no. 2, pp. 357–364, Apr. 2000.

[17] D.P. McNamara, M.A. Beach, P.N. Fletcher, and P. Karlsson, "Initial Investigation of Multiple-Input Multiple-Output Channels in Indoor Environments," in *IEEE Benelux Chapter Symp. Commun. Veh. Technol.*, Oct. 2000, Lueven, Belgium.

[18] D.P. McNamara, M.A. Beach, P.N. Fletcher, and P. Karlsson, "Temporal Variation of MIMO Channels in Indoor Environments," in *IEE Int. Conf. Antennas Propagat.*, Apr. 2001, Manchester, UK.

[19] D.P. McNamara, M.A. Beach, P.N. Fletcher, and P. Karlsson, "Capacity Variation of Indoor Multiple-Input Multiple-Output Channels," *IEE Electronics Letters*, vol. 36, no. 24, pp. 2037–2038, Nov. 2000.

[20] K. Wong, R.D. Murch, and K.B. Letaief, "Optimizing Time and Space MIMO Antenna System for Frequency Selective Fading Channels," *IEEE J. Select Areas Commun.*, vol. 19, no. 7, pp. 1395–1407, July 2001.

[21] J. Medbo and P. Schramm, "Channel Models for Hiperlan/2 in Different Indoor Scenarios," ETSI/BRAN Document No. 3ERI085B, Mar. 1998.

[22] J.G. Proakis, *Digital Communications*, McGraw-Hill, 3rd edition, 1995.